

ppi 201502ZU4659

This scientific digital publication is
continuance of the printed journal impresa
p-ISSN 0254-0770/ e-ISSN 2477-9377 / Legal
Deposit pp 197802ZU3



REVISTA TÉCNICA

DE LA FACULTAD DE INGENIERÍA

An international refereed Journal
indexed by:

- SCOPUS
- SCIELO
- LATINDEX
- DOAJ
- MIAR
- REDIB
- AEROSPACE DATABASE
- CIVIL ENGINEERING ABTRACTS
- METADEX
- COMMUNICATION ABSTRACTS
- ZENTRALBLATT MATH, ZBMATH
- ACTUALIDAD IBEROAMERICANA
- BIBLAT
- PERIODICA
- REVENCYT

UNIVERSIDAD DEL ZULIA



REVISTA TÉCNICA
DE LA FACULTAD DE INGENIERÍA

La Ciega Historical building. LUZ first headquarter

“Post nubila phoebus”
“After the clouds, the sun”

LUZ in its 130th
anniversary
Established since
1891

Relationship between SAW Coatings Composition and The Composition of Fluxes Obtained with Steel Slag and Rice Husk Ashes

R. Najarro¹, A. Cruz-Crespo^{2*}, L. Perdomo², A. Duffus², G. Almeida²,
M. J. Morales¹

¹ Universidad Técnica de Cotopaxi-La Maná, Av. Los Almendros y calle Pujili sector La Virgen, La Maná - Ecuador.

² Centro de Investigaciones de Soldadura, Facultad de Ingeniería Mecánica e Industrial, Universidad Central “Marta Abreu” de Las Villas, CP 54 830, Santa Clara, Cuba.

*Corresponding author: acruz@uclv.edu.cu

<https://doi.org/10.22209/rt.v44n2a06>

Received: 19 July 2020 | Accepted: 30 March 2021 | Available: 30 April 2021

Abstract

Submerged arc welding (SAW) surfacing is frequently applied on parts that work in abrasive wear conditions. The applied commercial fluxes are obtained from natural minerals. The objective of this work is to establish the relationship between the chemical composition of the alloy deposited by SAW and the composition of the flux, obtained from steel refining slag with the addition of rice husk ashes. Fluxes were obtained by pelletizing, based on a McLean-Anderson type design. Deposits were obtained with the experimental fluxes, which were chemically characterized. Empirical models of the element's composition in the deposited metal as function of the flux composition were developed, and an optimization process was carried out. It is concluded that the contents of the elements in the deposited metal show a quadratic dependence, the carbon content (C) is ruled by graphite composition in the flux, while the chromium (Cr), manganese (Mn) and silicon (Si) contents are ruled by the FeCrMn content.

Keywords: abrasive wear; hardfacing; SAW fluxes; steel slags.

Vínculo de la Composición de Recubrimientos SAW con la Composición de Fundentes Obtenidos con Escoria de Acería y Cenizas de Cascarilla del Arroz

Resumen

El recargue por soldadura con arco sumergido (SAW, según sus siglas en inglés) se aplica con frecuencia en piezas que trabajan en condiciones de desgaste abrasivo. Los fundentes comerciales que se utilizan son obtenidos a partir de minerales naturales. El objetivo del presente trabajo fue establecer los vínculos entre la composición química de la aleación depositada por SAW y la composición del fundente, elaborado a base de escoria de afino del acero con adición de cenizas de cascarilla del arroz. Se elaboraron fundentes por peletización con base en un diseño de tipo McLean-Anderson. Con los fundentes experimentales se obtuvieron depósitos, que fueron caracterizados químicamente. Se obtuvieron modelos de la composición de los elementos en el metal depositado en función de la composición del fundente y fue realizado un proceso de optimización. Se concluye, que los contenidos de los elementos en el metal depositado muestran una dependencia cuadrática, siendo el contenido de carbono (C) gobernado por el de grafito en el fundente, mientras los contenidos de cromo (Cr), manganeso (Mn) y silicio (Si) son gobernados por el contenido de FeCrMn.

Palabras clave: desgaste abrasivo; escorias de acería; fundente para SAW; recargue duro.

Introduction

Hardfacing by submerged arc welding (SAW) is frequently applied to reduce wear, since it offers a wide range of possibilities in varying the composition of the deposits and high productivity of the deposition process (Tusek and Suban, 2003; Gulenç and Kahraman, 2003; Shan-Ping et al., 2004; Mendez et al., 2014).

Almost all SAW fluxes are manufactured from natural minerals. However, the use, of steel welding slags by SAW, as raw material, is reported (Singh and Pandey et al., 2009). In the aforementioned work, welding slags of steels by SAW process are used to obtain a new agglomerated flux, also destined for the welding of steel structures. In previous publications by some of the authors of this work slags of the $\text{SiO}_2\text{-MnO}$ system resulting from the SAW welding of steel structures, and slags of the $\text{Al}_2\text{O}_3\text{-MgO-SiO}_2$ system from obtaining ferrochrome and ferrochromomanganese, were used as matrix component of a flux for SAW surfacing (Cruz-Crespo et al., 2005; Cruz-Crespo et al., 2017; Perdomo-González et al., 2017; Cruz-Crespo et al., 2019).

On the other hand, the steelmaking slags are characterized by the majority presence of the $\text{CaO-SiO}_2\text{-MgO-Al}_2\text{O}_3$ quaternary system. The greatest use of these slags has been focused on civil construction applications. Slag from the oxidation period during steelmaking, due to their relatively high Fe_2O_3 and P_2O_5 contents, are not viable for the production of fluxes. However, the slags from the steel refining process are suitable as raw material for the production of SAW fluxes, since these slags practically do not contain Fe_2O_3 and P_2O_5 (Najarro-Quintero et al., 2018a).

Rice husk constitutes an agroindustrial residual to which no systematic treatment has been found, despite the fact that many authors report the potential of its ashes for its use in the development of new materials, especially due to its pozzolanic properties (Jarre et al., 2021).

In previous studies by the authors of the present work, the use of steel refining slags as a component of the matrix of a flux for surfacing by SAW was validated, also validating the addition of rice husk ash to incorporate SiO_2 to the matrix system. (Najarro-Quintero et al., 2018a; Najarro-Quintero et al., 2018b). The present work is a continuity of the referred studies, when considering as objective, to establish the links between the flux composition variables and the chemical composition of the alloy deposited by SAW, based on a mixtures experimental design for a restricted region.

Experimental

A McLean-Anderson type experimental design was applied in the study, considered as independent variables, the flux matrix (X_1), the graphite (X_2) and the FeMnCr (X_3). In flux, graphite and FeCrMn constitute the alloying system. The experimental matrix (Table 1) was obtained as follows: From the complete design matrix (12 possible combinations of variables), and after applying the normality condition $\sum X_i = 100\%$ and eliminating the points with variables out of range; as well as when considering the coincident experimental points, only 4 valid experiments remained (a, b, c, d). Between these points, 4 new points were added (ab, bc, cd, da) and one in the center (abcd).

To obtain each experimental flux the mixture of matrix components was prepared. The composition of the flux matrix was established in a previous study (Najarro-Quintero et al., 2018a), and its percentage ratio of components is: 72.99 % slag from the ACINOX Las Tunas ladle furnace, 20.44 % ash from rice husk combustion and 6.57 % fluorite. The matrix components were brought to a granulometry of less than 0.25 mm; while FeCrMn and graphite were ground and sieved in a range between 0.1 and 0.25 mm. The compositions of the raw materials used to obtain the experimental fluxes are shown in Table 2.

The loads of 1 kg, corresponding to each experimental flux (Table 1), were dosed by weighing on a technical balance. To guarantee the homogeneity of the loads they were mixed in a rotating drum for 30 min. Agglomeration was carried out by pelletizing, using sodium silicate, as binder, in a proportion of 30 % of the dry mass. The fluxes obtained were air-dried, then sieved to a particle's size between 0.25 and 2.0 mm, and finally calcined in a muffle furnace at 350 °C for 120 min. The percentage composition of the flux components, considering the addition of 30 % sodium silicate, is shown in Table 1. The addition of 30 % sodium silicate ($\text{SiO}_2\text{-}29.39$; $\text{Na}_2\text{O-}$

10.10 and H₂O - 60.51 %), provides 11.85 g of (SiO₂ + Na₂O) for 100 g of the flux dry mass (matrix + graphite + FeCrMn), since the water is evaporated during the calcination process, representing 10,59% the contribution of silicate on the flux (Table 1).

Table 1. Experimental matrix and composition of agglomerated fluxes, % in mass.

Experimental matrix				Agglomerated flux			
Experiment	X ₁	X ₂	X ₃	Matrix	Graphite	FeCrMn	SiO ₂ + Na ₂ O
a	88	7.0	5.0	78.68	6.26	4.47	10.59
b	88	2.0	10.0	78.68	1.79	8.94	10.59
c	78	2.0	20.0	69.74	1.79	17.88	10.59
d	78	7.0	15.0	69.74	6.26	13.41	10.59
ab	88	4.5	7.5	78.68	4.02	6.71	10.59
bc	83	2.0	15.0	74.21	1.79	13.41	10.59
cd	78	4.5	17.5	69.74	4.02	15.65	10.59
da	83	7.0	10.0	74.21	6.26	8.94	10.59
acbd	83	4.5	12.5	74.21	4.02	11.18	10.59

Table 2. Chemical composition, in mass %, of flux filler components.

Flux matrix components							
	SiO ₂	CaO	CaF ₂	CO ₂	SO ₃	P ₂ O ₅	Others
Ash, %	90-97	*	-	-	-	-	*
Fluorite, %	2.87	1.12	95.00	0.88	0.10	0.03	-
Flux alloy load components							
	Cr	Mn	C	Si	S	P	Fe
FeCrMn	19.45	59.02	0.11	2.17	0.0036	0.17	balance
Graphite	-	-	99.00	-	-	-	-

* Variable contents of the oxides of Ca, Mg, K, Na, Al, Fe, etc., depending on the characteristics of the soils (Cruz, 2009), -: compound or element not present in the raw material.

Deposits, with experimental fluxes, were made on AISI 1020 steel plates with dimensions 150x80x8 mm. AWS EL12 electrode wire of 3 mm was used, with a current of 300 A, an arc voltage of 35 V, a welding speed of 43.2 m/h and a flux layer's height of 20 mm. The deposit was obtained in three superimposed layers. From each deposit, a sample was extracted for chemical analysis, by cross section cuts in a metallographic cutter. The composition was determined by atomic emission spectroscopy.

The result processing was carried out with the Statgraphics software, obtaining the regression equations of C, Cr, Mn and Si contents in the deposited metal, as a function of the input experimental design variables. A multivariable optimization process was also carried out to define the deposit with the best composition in terms of abrasive wear.

Results and Discussion

The average chemical composition values of the fundamental elements of the deposits are shown in Table 3. Equations 1, 2, 3 and 4 reflect the behavior of the C, Cr, Mn and Si contents in the deposited metal, depending on the flux composition variables. In all cases, the behavior is quadratic, with a high adjustment of the models for C, Cr and Mn: R² = 96.84 % and adjusted R² = 91.56 % (p = 0.0186) for C, R² = 99.00 % and adjusted R² = 97.34 % for Cr (p = 0.0034), R² = 98.33 % and adjusted R² = 95.56 % (p = 0.0072) for Mn. The Si model did not show a high adjustment (R² = 89.63 %, adjusted R² = 72.35 % and p = 0.1030); however, regularity is observed for a probability of around 90 %, which makes it possible to evaluate the behavioral trend.

Table 3. Composition of the experimental deposits, contribution of the flux-wire system and transfer coefficients of the elements to the deposited metal.

Deposits composition (%)					Contribution of the flux-wire system (%)				Transfer coefficients			
Flux	C	Mn	Cr	Si	C	Mn	Cr	Si	K_{tC}	K_{tMn}	K_{tCr}	K_{tSi}
a	2.53	1.00	0.38	1.26	4.00	1.87	0.56	0.10	0.63	0.54	0.68	12.85
b	0.65	2.87	0.95	1.43	1.17	3.56	1.11	0.16	0.55	0.81	0.85	8.93
c	0.77	4.80	1.34	2.59	1.18	6.93	2.23	0.28	0.65	0.69	0.60	9.11
d	2.83	3.92	1.07	2.29	4.01	5.25	1.67	0.22	0.71	0.75	0.64	10.30
ab	2.01	1.87	0.73	2.36	2.59	2.71	0.83	0.13	0.78	0.69	0.87	18.28
bc	1.00	3.71	1.11	2.11	1.17	5.25	1.67	0.22	0.85	0.71	0.66	9.49
cd	1.73	5.05	1.40	3.06	2.59	6.09	1.95	0.25	0.67	0.83	0.72	12.08
da	2.50	2.33	0.73	2.16	4.00	3.56	1.11	0.16	0.62	0.66	0.66	13.49
abcd	2.09	3.67	1.12	2.33	2.59	4.40	1.39	0.19	0.81	0.83	0.81	12.19

K_{tC} , K_{tMn} , K_{tCr} , K_{tSi} : transfer coefficients of C, Mn, Cr and Si, respectively.

$$C = 0.483333 * X_1 + 0.938333 * X_2 + 0.748333 * X_3 + 8.46 * X_1 * X_2 + 0.99 * X_1 * X_3 + 8.28 * X_2 * X_3, \quad (1)$$

$$Cr = 0.672222 * X_1 - 3.10278 * X_2 + 1.34722 * X_3 + 4.245 * X_1 * X_2 + 0.075 * X_1 * X_3 + 5.52 * X_2 * X_3, \quad (2)$$

$$Mn = 1.66167 * X_1 - 7.95583 * X_2 + 4.88917 * X_3 + 10.71 * X_1 * X_2 - 0.135 * X_1 * X_3 + 15.3 * X_2 * X_3, \quad (3)$$

$$Si = 0.898333 * X_1 - 12.7092 * X_2 + 2.54583 * X_3 + 22.86 * X_1 * X_2 + 0.315 * X_1 * X_3 + 21.96 * X_2 * X_3, \quad (4)$$

The response surfaces (Figures 1, 2, 3 and 4), corresponding to the regression equations (Equations 1, 2, 3 and 4), show the behavior trend. It is observed, as expected, that with the increase of graphite content in the alloying system of the flux, the C content in the deposited metal tends to increase too. Similarly, the Cr and Mn contents in the deposits tend to be higher, as the FeCrMn content in the flux increases. In the case of Si, the growth tendency is governed by the addition of FeCrMn (X_3), because this component of the flux alloy system directly adds Si, while Mn acts as a deoxidizer, favoring the SiO_2 reduction.

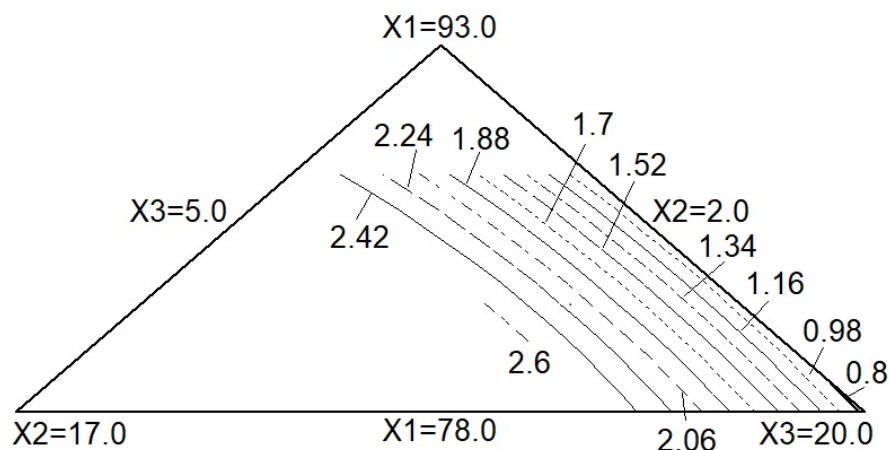


Figure 1. Isolines of surfaces responses of the C content in the deposit (%), as a function of the matrix (X_1), graphite (X_2) and FeCrMn (X_3) contents in the flux (%).

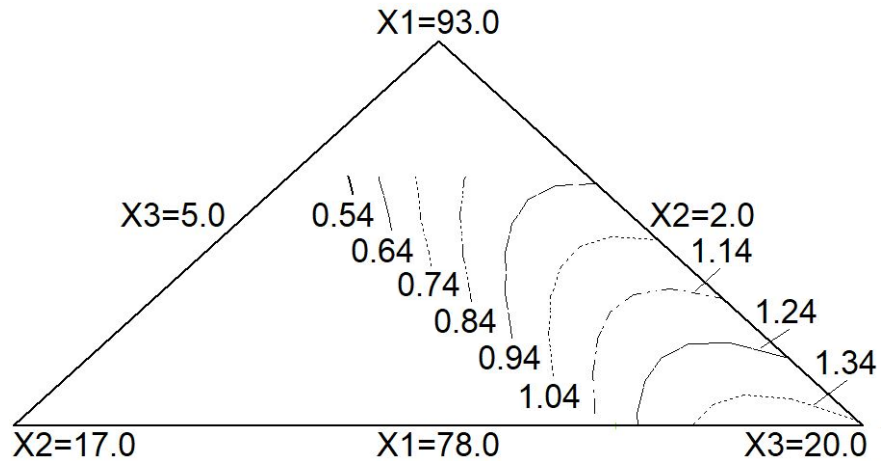


Figure 2. Isolines of response surfaces of the Cr content in the deposit (%), as a function of the matrix (X_1), graphite (X_2) and FeCrMn (X_3) contents in the flux (%).

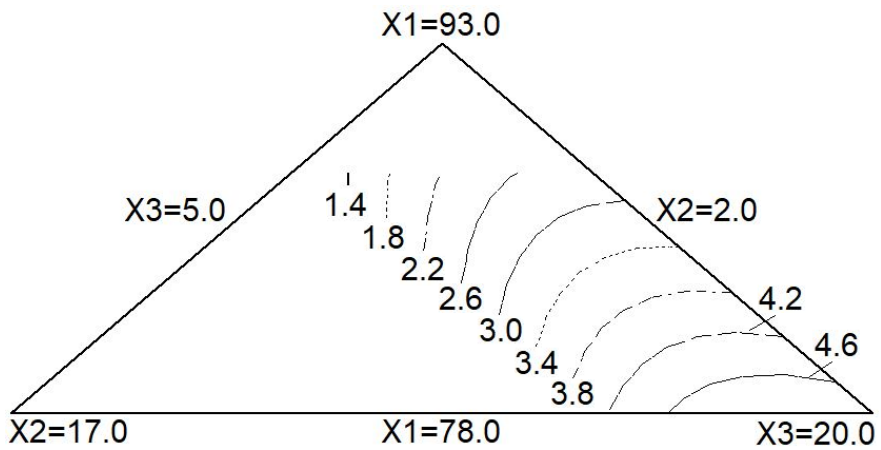


Figure 3. Isolines of surface responses of the Mn content in the deposit (%), as a function of the matrix (X_1), graphite (X_2) and FeCrMn (X_3) contents in the flux (%).

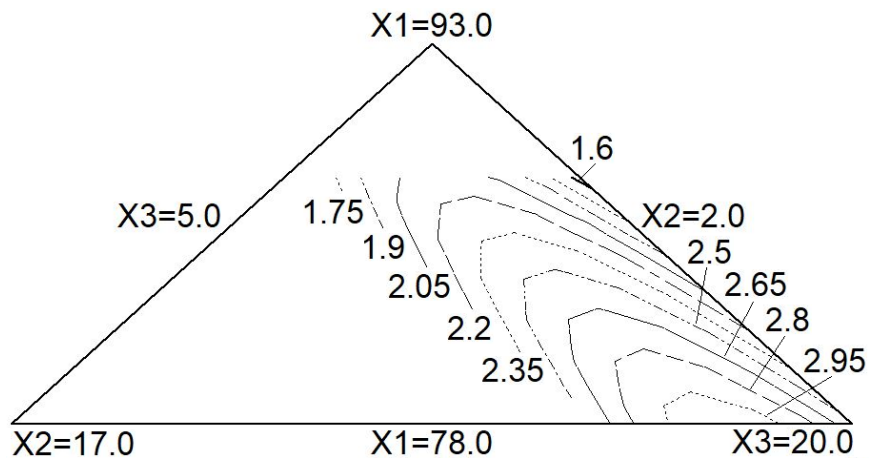


Figure 4. Isolines of surfaces responses of the Si content in the deposit (%), as a function of the matrix (X_1), graphite (X_2) and FeCrMn (X_3) contents in the flux (%).

The chemical composition described in Table 3, recalculated to 100 % of the Fe-Cr-C ternary system, shows that in all deposits the primary crystallization of the melting pool occurs with the formation of austenite (Albertin et al., 2011). Due to the high cooling rates, typical of a welding surfacing process, austenite transforms to martensite. Cr and Mn, which are carbide formers, shift the isothermal transformation curves of austenite to the right, while lowering the starting point of the martensitic transformation, which cause the appearance of residual austenite. Given the chemical composition (Table 3) and the microstructure resulting from cooling, the experimental deposits are relatively similar to those provided by commercial consumables recommended for abrasive wear (AWS A 5.13, 2014; Kobe, 2007).

Analysis of the deposits alloying process

Table 3 shows the contribution of alloying elements of each flux, in combination with the AWS EL12 wire. The contribution was determined based on the chemical composition of the alloy load components (Table 2) and their proportions in the conformation of the experimental fluxes, considering the contribution of sodium silicate, used as a binder (Table 1). In determining the contribution of elements to the deposit by the flux-wire system, it was considered that the composition of the AWS EL12 electrode wire is: C-0.09 %; Mn-0.5 %; Si-0.1 % (AWS A 5.17, 2001) and that the flux/wire consumption ratio is around 1.8 (of the total consumption, the flux represents 64 % and the wire 36 %).

When comparing the contributions of the flux-wire system with the composition of the experimentally deposited metal (Table 3 and Figure 5), it is observed that there is relative correspondence for Cr, Mn and C. The contribution of the wire-flux system differs of the composition of deposits, since oxidation-reduction processes take place during deposition. The tendency to a certain linearity in the behavior between the contribution of the flux-wire system and the experimental composition obtained in the deposits (Figure 5), shows that the concentration conditions govern the metal alloying, despite the high cooling rates that take place in SAW surfacing, which can lead the system to thermodynamic imbalance.

The Si contents in the experimental deposits significantly exceed the values of this element provided by the flux-wire system (Table 3). This is caused by the silica reduction (Equation 5) in the high temperature zones (in the drop and the front zone of the weld pool). The [FeO] dissolved in the liquid metal reacts with the [Mn] and [C], contained in the pool, according to the reactions of Equations 6 and 7, releasing iron and favoring the reduction of SiO₂ at the metal-slag interface by Equation 5 (Quintana et al., 2003). The high SiO₂ content in the weld slag, provided by the flux matrix (SiO₂ is provided by the steel slag, by the ash and by the sodium silicate), and the presence of Mn and C that act as deoxidizers (Equations 6 and 7), favor the reaction of Equation 5, which leads to the increase of this element in the metal. Namely:



Based on the content of elements provided by the flux-wire system and the composition of the deposits obtained experimentally, the transfer coefficients of the elements were determined ($K_{IE} = E_{exp}/E_{theoretical}$; K_{IE} - transfer coefficient of the element to the deposited metal, E_{exp} and $E_{theoretical}$ - experimental and theoretical contents of the element in the deposited metal) (Table 3). The transfer coefficient reflects the effective use of the alloying element, provided by the consumables to obtain the deposited metal. In the case of C, Mn and Cr, since the values are lower than one, it is confirmed that there are losses related to the oxidation of these elements. The C and Mn transfer coefficient values, in a general exceed those frequently reported in the literature; while Cr transfer coefficient is in the range reported by literature, with only two values higher than said range (Potapov, 1989; Quintana et al., 2003). In the case of Si, in correspondence with what has already been discussed about the reduction of SiO₂, the transfer

coefficient is significantly higher than one, evidencing that there has been incorporation of this element into the deposit, after a reductive process of the oxide from the slag, according to Equation 5.

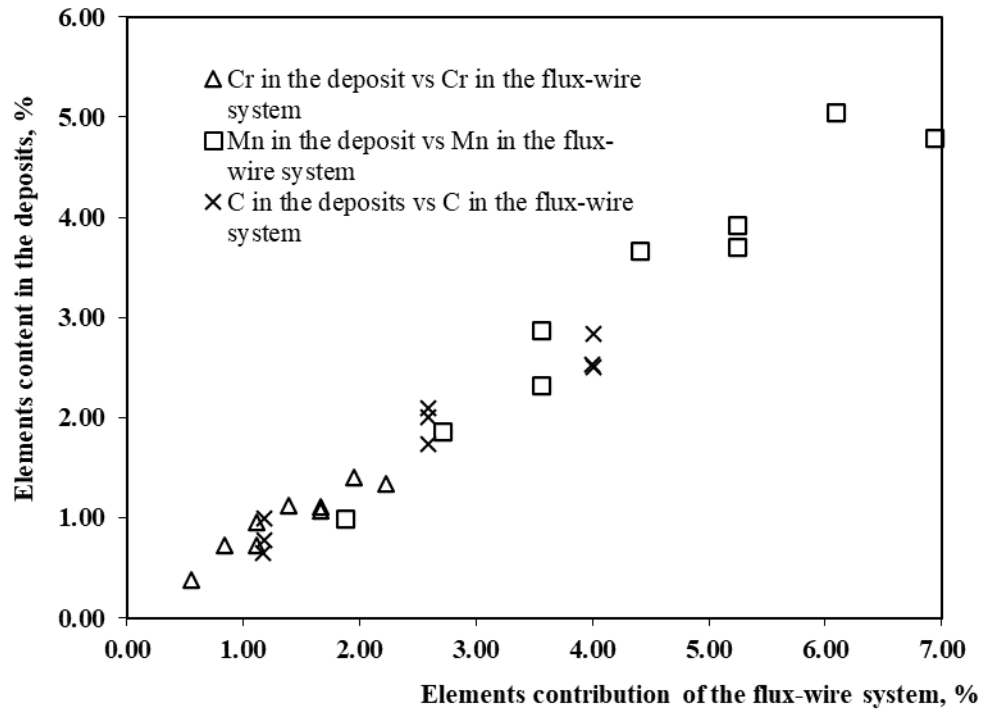


Figure 5. Relationship between the contents of the alloying elements in the flux-wire system and in the deposited metal.

The similar trend behavior of the Cr and Mn contents in the deposited metal (Figures 2 and 3), being these elements added by the same load component of the flux (FeCrMn, identified as the variable X_3 in the experimental plan, Table 1), shows that the deposit alloying is governed by the concentration conditions.

In the case of C, due to the relatively low amount of atmospheric oxygen and the high temperatures in the arc, its oxidation occurs predominantly with the oxides in the liquid metal (Quintana et al., 2003).

Flux composition optimization

As already stated, all the deposits obtained with the experimental fluxes in combination with AWS EL12 wire (Table 3), could satisfy the requirements for abrasive wear. However, from the point of view of the deposited metal composition, the C and Cr contents should be the highest possible, since this favors the formation of hard structures that limit the penetration of the abrasive material on the coating surface. The independent optimization of these two responses (C and Cr in the deposited metal), through processing with the Statgraphics software, provides the following: $C_{opt} = 2.7\%$ ($X_1 = 81.45$; $X_2 = 7.0$ and $X_3 = 11.55\%$); $C_{ropt} = 1.4\%$ ($X_1 = 78.0$; $X_2 = 3.45$ and $X_3 = 18.55\%$). The foregoing shows that the best results of the C and Cr content in the deposit are not coincident, in terms of composition of the flux, so it is necessary to find a compromise condition, which can be achieved by obtaining the function of desirability (Becerra et al., 2014).

Multivariable optimization processing was done, maximizing C and Cr as responses. As a result, the graph of the “desired” function has been obtained (Figure 6). It is observed that the best results tend towards an increase in graphite and a decrease in the matrix with high FeCrMn values, the optimum of the “desired” function being equal to 0.82, which corresponds to the following: $C_{opt} = 2.45$ and $Cr_{opt} = 1.22\%$ ($X_1 = 78.0$; $X_2 = 6.12$ and $X_3 = 15.88\%$). This optimum coincides with the experimental point “d” (Table 1). Due to its composition, this deposit could satisfy the requirements for abrasive wear, corresponding to the AWS EFe5 classification, according to what was reported

for welding surfacing consumables (AWS A 5.13, 2010). The Mn in the deposit contributes to the presence of residual austenite, which is favorable under abrasion with impact conditions.

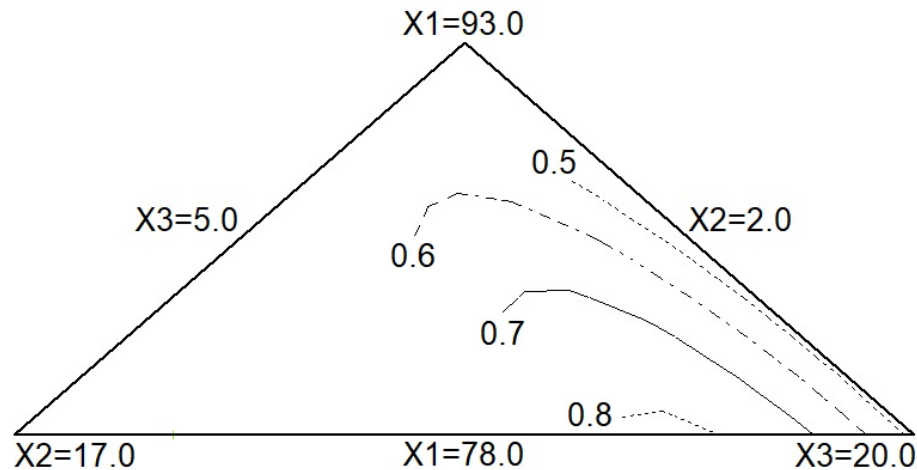


Figure 6. Behavior of the "desired" function, depending on the matrix (X_1), graphite (X_2) and FeCrMn (X_3) contents in the flux (%).

The hardness of the deposit obtained with the flux "d" (549 HV, 53 HRc) and the microstructure shown in Figure 7, with the presence of needle-shaped martensite and residual austenite, indicate that the flux selected as optimal, could be suitable for abrasive wear. Several authors, among which are Gulenc and Kahraman (2003), and Coronado et al. (2009), carried out studies that validate the performance on abrasive wear of steels coatings, with a similar composition and microstructure of the deposits in the present work.

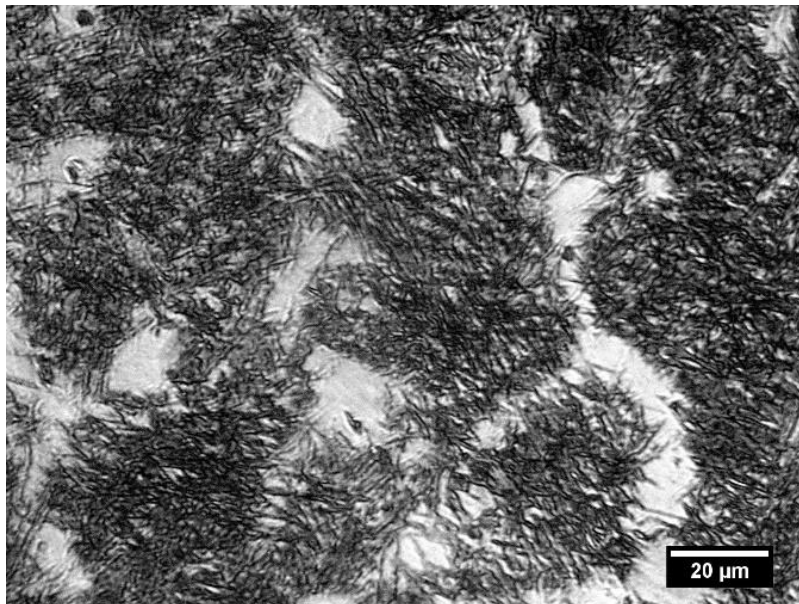


Figure 7. Microstructure of deposit "d" obtained by optical microscopy (needle-shaped martensite-dark area and austenite-light area).

Conclusions

It is confirmed that slags from the steel refining process, with rice husk ashes as an additive, are viable to use as matrix components of alloyed agglomerated fluxes for surfacing by SAW process.

The C, Cr, Mn and Si contents in the deposited metal, as a function of the matrix, graphite and FeCrMn contents in the fluxes, show a quadratic dependence. The graphite content in the flux governs the C content in the deposits, while the Cr, Mn and Si content are governed by the FeCrMn content in the flux. The transfer of C, Cr and Mn to the deposit, from the flux-wire system, is manifested with losses due to the oxidation processes of these elements, while the Si content in the deposited metal is higher than that provided, due to the reduction of SiO₂ present in the slag.

The compositions of the deposits obtained with the experimental fluxes are in similar ranges to those of commercial consumables for abrasive wear, characterized by the predominance of martensite in the microstructure and the presence of residual austenite. From the optimization process to maximize C and Cr, the flux with the best properties is similar to the experimental "d" and is characterized by C_{opt} = 2.45 and Cr_{opt} = 1.22 % (X₁ = 78.0; X₂ = 6.12 and X₃ = 15.88 %), with hardness around 53 HRc.

References

- Albertin, E., Neto, F. B., Teixeira, I. O. (2011). Adequação da composição química e do tratamento térmico de ferros fundidos de alto cromo utilizando termodinâmica computacional. *Tecnol. Metal. Mater. Miner.*, 8(4), 223-229.
- AWS A 5.13. (2010). *Specification for surfacing electrodes for shielded metal arc welding*. Miami: American Welding Society.
- AWS A5.17. (2001) *Specification for carbon steel electrodes and fluxes for Submerged Metal Arc Welding*. Miami: American Welding Society.
- Becerra, M. B., Zitzumbo, R., Domínguez J., García, J. L., Alonso, S. (2014). Use of the desirability function to optimize a vulcanized product. *Rev. Téc. Ing. Univ. Zulia*, 37(1), 85-94.
- Cruz-Crespo, A., Quintana-Puchol, R., García, L. L., Perdomo, L., Jiménez, G., Gómez, C. R., Alguacil, F. J., Cores, A. (2005). Empleo de escorias de soldadura del sistema MnO-SiO₂ para la obtención de un nuevo fundente aglomerado aleado. *Rev. Metal.*, 41(1), 3-11.
- Cruz-Crespo, A., Perdomo-González, L., Fernández, R., Scotti, A. (2017). Composición química y microestructura del metal depositado con fundentes obtenidos con empleo de escorias del sistema MnO-SiO₂-CaO^o. *CentroAzucar*, 44(3), 43-52.
- Cruz-Crespo, A., Perdomo-González, L., Quintana-Pucho, R., Scotti, A. (2019). Fundente para recargue por soldadura con arco sumergido a partir de ferrocromo-manganeso y escoria de la reducción simultánea de cromita y pirolusita. *Soldagem & Inspeção*, 24, 1-10.
- Gulenç, B., Kahraman, N. (2003). Wear behaviour of bulldozer rollers welded using a submerged arc welding process. *Materials and Design*, 24, 537-542.
- Jarre, C. M., Puig, R. A., Zamora-Ledezma C., Zamora-Ledezma, E. (2021). Caracterización preliminar de la ceniza de cáscara de arroz de la provincia Manabí, Ecuador, para su empleo en hormigones. *Rev. Téc. Ing. Univ. Zulia*, 44(1), 44-50.
- John J. Coronado, J. J., Caicedo H. F., Gómez, A. L. (2009). The effects of welding processes on abrasive wear resistance for hardfacing deposits. *Tribology International*, 42, 745-749.
- Kobe, S. (2007). Types of wear and suitable hardfacing filler metals. *Kobelco Welding Today*, 10(3), 3-7.

- Mendez, P. F., Barnes, N., Bell, K., Borle, S. D., Gajapathi, S. S., Guest, S. D., Izadi, H., Gol, A. K., Wood, G. (2014). Welding processes for wear resistant overlays. *Journal of Manufacturing Processes*, 16, 4-25.
- Najarro-Quintero, R., Cruz-Crespo, A., Perdomo-González, L., Ramírez-Torres, J., Orbea-Jiménez M. (2018a). Empleo de escorias de horno cuchara y de cenizas de paja de arroz como componentes de un fundente para recargue por soldadura. *Minería y Geología*, 34(3), 331-344.
- Najarro-Quintero, R., Cruz-Crespo, A., Perdomo-González, L., Ramírez-Torres, J., López R. (2018b). Potencialidades de las escorias de afino del acero en la obtención de un fundente para recargue por soldadura. *CentroAzucar*, 45(4), 32-40.
- Perdomo-González, L., Quintana-Puchol, R., Cruz-Crespo, A., Gómez-Pérez, C. R. (2017). Obtaining of components of fluxes for submerged arc welding from the carbothermic reduction of chromite refractory. *Rev. Téc. Ing. Univ. Zulia*, 40(1), 42-51.
- Potapov, N. N. (1989). *Materiales para soldar: Gases protectores y fundentes*. Moscú: Mashinoestroyeniye.
- Quintana, R., Cruz, A., Perdomo, L., Castellanos, G., García, L. L., Formoso, A., Cores A. (2003). Eficiencia de la transferencia de elementos aleantes en fundentes durante el proceso de soldadura automática por arco sumergido. *Rev. Metal.*, 39(1), 25-34.
- Shan-Ping, L., Oh-Yang, K., Tae-Bum, K., Kwon-Hu, K. (2004). Microstructure and wear property of Fe–Mn–Cr–Mo–V alloy cladding by submerged arc welding. *Journal of Materials Processing Technology*, 147, 191-196.
- Singh, K., Pandey, S. (2009). Recycling of slag to act as a flux in submerged arc welding. *Resources, Conservation and Recycling*, 53, 552-558.
- Tusek, J., Suban, M. (2003). High-productivity multiple-wire submerged-arc welding and cladding with metal-powder addition. *Journal of Materials Processing Technology*, 133, 207-213.



UNIVERSIDAD
DEL ZULIA

REVISTA TECNICA

OF THE FACULTY OF ENGINEERING
UNIVERSIDAD DEL ZULIA

Vol. 44. N°2, May - August, 2021 _____

*This Journal was edited and published in digital format
on April 2021 by **Serbiluz Editorial Foundation***

www.luz.edu.ve
www.serbi.luz.edu.ve
www.produccioncientificaluz.org